Title
Photochemistry of aldehyde clusters: cross-molecular versus unimolecular reaction dynamics

Journal
Physical Chemistry Chemical Physics, 16(43)

ISSN
0956-5000

Authors
Shemesh, Dorit
Blair, Sandra L
Nizkorodov, Sergey A
et al.

Publication Date
2014-11-21

DOI
10.1039/c4cp03130j

PCCP

PAPER

View Article Online
View Journal | View Issue

Cite this: *Phys. Chem. Chem. Phys.*, 2014, **16**, 23861

Photochemistry of aldehyde clusters: cross-molecular *versus* unimolecular reaction dynamics

Dorit Shemesh,[a] Sandra L. Blair,[b] Sergey A. Nizkorodov[b] and R. Benny Gerber*[abc]

Received 16th July 2014,
Accepted 16th September 2014

DOI: 10.1039/c4cp03130j

www.rsc.org/pccp

The unimolecular photochemistry of aldehydes has been extensively studied, both experimentally and computationally. However, less is known about the role of cross-molecular photochemical processes in the condensed-phase photolysis of aldehydes. The triplet-state photochemistry of pentanal in its pentameric (n = 5) cluster was investigated as a model for photochemical reactions of aliphatic aldehydes in atmospheric aerosols. This study employs "on the fly" dynamics simulations using a semi-empirical MRCI electronic code for the singlet and triplet states involved. Previous studies have shown that the triplet-state photochemistry of an isolated pentanal molecule is dominated by Norrish I and II reactions. The main findings for the cluster are: (1) 55% of the trajectories lead to a unimolecular or cross-molecular reaction within a timescale of 100 ps; (2) cross-molecular reactions occur in over 70% of the reactive trajectories; (3) the main cross-molecular processes involve an H-atom transfer from the CHO group of the excited pentanal to an O atom of a nearby pentanal; and (4) the unimolecular Norrish II reaction is suppressed by the cluster environment. The predictions are qualitatively supported by experimental results on the condensed-phase photolysis of an aliphatic aldehyde, undecanal. The computational approach should be useful for predicting the mechanisms of other condensed-phase organic photochemical reactions. These results demonstrate a major role of cross-molecular processes in the condensed-phase photolysis of carbonyls. The cross-molecular reactions discussed in this work are relevant to photolysis-driven processes in atmospheric organic aerosols. It is expected that the condensed-phase environment of an organic aerosol particle should support a multitude of similar cross-molecular photochemical processes.

I. Introduction

Chemical kinetics and dynamics of unimolecular reactions of isolated molecules in the gas phase are well understood.[1,2] The framework of a unimolecular process is often applied, at least as an idealization, to condensed phase processes although the effects of the environment on the process can be profound.[3] A good example is photodissociation of small molecules, such as HCl or F_2, in noble gas matrices and clusters.[4,5] Photodissociation in such systems is strongly affected by cage effects that greatly alter the process.[6,7]

Matrix effects become more complex and harder to characterize and understand when the medium is molecular, such as an organic solvent. Situations where reactions with neighboring solvent molecules may take place greatly complicate the understanding of the relative roles of unimolecular and cross-molecular processes. Only in relatively few cases has a detailed, quantitative understanding of the connection between unimolecular and cross-molecular reactions in a molecular medium been established so far. Some of the best-studied cases to date are photo-induced reactions in small molecular clusters. For example, Wittig and co-workers studied the photolysis of hydrogen halides HX in $HX\cdots CO_2$ complexes, and discovered an important role of the intermediate HOCO in these processes.[8,9] Zewail and co-workers explored the dynamics of these reactions by ultrafast laser techniques and directly measured the timescales of these processes.[10,11] Evidence of a cross-molecular reaction was found in a study of photodissociation of HCl in its dimer, $(HCl)_2$.[12] In contrast to these relatively small systems, unraveling the dynamics of cross-molecular *versus* unimolecular reactions in larger systems remains a major challenge. Our main objective is to explore the relative roles of unimolecular and cross-molecular reactions for a carbonyl photodissociation process involving relatively large molecules and predict whether these cross-molecular reactions play an important role in organic and atmospheric photochemistry.

[a] *Institute of Chemistry and the Fritz Haber Research Center, The Hebrew University of Jerusalem, Jerusalem 91904, Israel. E-mail: benny@fh.huji.ac.il*
[b] *Department of Chemistry, University of California, Irvine, CA 92697-2025, USA*
[c] *Laboratory of Physical Chemistry, FIN-00014 University of Helsinki, P.O. Box 55, Finland*

We have chosen pentanal, an aliphatic aldehyde, as a model system to explore the role of cross-reactions in condensed-phase photolysis. Carbonyl compounds are widespread in the atmosphere. Certain carbonyls are directly emitted by various sources, but the vast majority of them are produced in the atmosphere by oxidation of hydrocarbons.[13] Photolysis is an important removal pathway for atmospheric carbonyls. In the lower atmosphere, where the availability of radiation is limited to a wavelength of above ~290 nm, the photolysis of carbonyls is driven by their weak absorption band in the wavelength range 240–360 nm as a result of a dipole forbidden $n \rightarrow \pi^*$ transition.[13,14] Photolysis of aldehydes, such as pentanal, is known to occur through the following pathways:

$$RCHO + h\nu \rightarrow RH + CO \quad (A)$$

$$\rightarrow R + HCO \quad (B)$$

$$\rightarrow R''{=}R' + CH_3CHO \quad (C)$$

$$\rightarrow RCO + H \quad (D)$$

Process A is the molecular fragmentation channel. Process B represents the fragmentation into two free radicals (Norrish type I splitting). Process C is called a Norrish type II splitting, and it results in acetaldehyde and an alkene as the products. Norrish type II splitting is only possible for aldehydes larger than butanal, and the reason pentanal was selected as the model for this work is to make sure this important channel is included in the calculation. Process D is an H-abstraction process and has been found to be minor in small aldehydes.[15] In the microscopic picture, the photoexcitation promotes the system to the first excited singlet state (S_1) of $n\pi^*$ character. The S_1 state can either switch to the ground S_0 state *via* internal conversion, or reach the lowest triplet state T_1 *via* intersystem crossing (ISC). There is evidence that process B can occur either in the ground state or in the triplet state.[16]

Previous studies on the photochemistry of aliphatic aldehydes at atmospherically relevant photolysis wavelengths focused on gas-phase photodissociation[16–30] and its pressure dependence.[31–35] Photolysis of aldehydes in a condensed matter environment, found for example in atmospheric aerosols, cloud and fog droplets, and in thin films formed on urban surfaces has not been systematically investigated. The extension of the experiments and computer simulations from a bare molecule to a condensed-phase environment presents a real challenge since additional molecules increase the complexity of the system, especially if cross-molecular reactions have to be treated explicitly. To overcome this challenge, we explore the photochemistry by studying a small cluster of pentanal molecules with the aim of reaching conclusions that will hopefully guide us towards understanding the behavior in more realistic condensed-phase systems such as aerosols. We do so by adopting a computational framework that allows for the occurrence of cross-molecular reactions. The structure of the article is as follows: in Section IIa we briefly survey the photochemical dynamics of pentanal, a typical medium-size aldehyde of atmospheric relevance. We outline in Section IIb the computational approach. Section III presents the computational results for the cluster and discusses the physical mechanisms. Section IV provides conclusions and future outlook.

II. Methodology

(a) Reactions of an isolated pentanal molecule

From our previous study on the photochemistry of an isolated pentanal molecule[26] we obtained the following insights into the mechanisms and timescales of the reactions on the lowest triplet state surface. The relative yields of the Norrish type I and II reactions were 34% and 66%, respectively, which is in good agreement with the experimentally observed values.[21,32] The third type of reaction observed was an ultrafast H-atom detachment; in the small number of trajectories resulting in the H-atom detachment it always occurred on the sub-picosecond timescale. Norrish type I reactions occurred in the timescale of up to 10 ps, whereas Norrish type II reactions mostly occurred after 20 ps.

Properties such as bond order and Mulliken charges confirmed that the $C–C_\alpha$ bond cleavage of the Norrish type I reaction is homolytic and that two radical fragments are produced. Norrish type II reactions involve an intramolecular H-atom transfer (as confirmed by Mulliken charges and bond orders). The molecule needs to undergo conformational changes until the right configuration for the H-atom transfer is reached. For this reason, the Norrish type II reaction occurs on a longer timescale than the Norrish type I reaction.

(b) Computational approach

Different approaches enable the investigation of photochemical processes, both on the singlet and triplet state surfaces.[36–43,71] Noteworthy in particular is the recent progress in non-adiabatic dynamics calculations on triplet-excited state potential energy surfaces.[43] However, for this system, there appears to be no crossing between different triplet state surfaces on the timescale of 100 ps, as verified in the previous study of the bare pentanal.[26] In the simulations reported here, classical trajectories are computed to describe the reaction process in time. The reliability of the potential surface is of critical importance for accurately capturing the dynamics of the reaction. Based on our experience with related processes,[26,44–46] a semiempirical orthogonalization-corrected Method 2 (OM2)[47] and OM2/MRCI (multireference configuration interaction)[48] was used. The efficiency of the method made possible the calculation of a substantial set of trajectories (100) sufficient to predict the yields of different reaction channels with reasonable accuracy.

A cluster size of five pentanal molecules was chosen due to the following considerations: first of all, a cluster of five pentanal molecules is small enough to permit calculations using the OM2/MRCI method. Secondly, the cluster is large enough to surround a pentanal monomer by neighboring molecules to an extent that the unimolecular reactions may be significantly affected. Lastly, it is estimated that a cluster of this size will be amendable to future experimental studies.

The structure of the pentanal cluster consisting of five pentanal molecules was optimized in the ground state by the semiempirical OM2 method. The OM2 method was successful in describing Norrish-I and Norrish-II reactions in an isolated pentanal molecule, the processes that can also be expected to occur in the pentanal cluster.[26] A related semiempirical method, Parameterized Model number 3 (PM3),[49] has been previously used for the first principles dynamics calculations for biologically and atmospherically relevant systems.[50–55] OM2 molecular dynamics simulation in the ground state of the pentanal cluster has shown that the cluster tends to evaporate within the short simulation time. To improve the method accuracy, dispersion corrections[56] were added in the dynamical simulations. These corrections kept the pentanal cluster intact during ground state molecular dynamics simulation. The dispersion correction by Wu and Yang[56] is described by the following dumping function:

$$f_D(R) = \frac{1}{\left(1 + \exp\left[-\beta\left(\frac{R}{R_m} - 1\right)\right]\right)}$$

where R is the distance between two atoms, R_m is the sum of the atomic vdW radii of the respective atoms, and β has an empirical value of 23.0.

Simulation of photoinduced processes in the pentanal cluster was carried out *via* excited-state dynamics calculations utilizing the semiempirical Modified Neglect of Diatomic Overlap (MNDO) program.[57,58] The simulation consisted of three steps: (1) ground-state dynamics to sample the initial configurations; (2) vertical transition to the first excited singlet state S_1 and ISC from S_1 to the lowest triplet state T_1; and (3) excited-state dynamics on T_1. The simulation scheme has been applied successfully in two similar systems, and is described in more details in ref. 26 and 46.

The sampling of the initial conditions was carried out by running a trajectory computed using the OM2 potential surface in the ground electronic state for 10 ps, at a temperature of 300 K. The velocity-Verlet algorithm with a time-step of 0.1 fs was employed. The significance of triplet electronic states in the photolysis of carbonyls is well established.[3] It was assumed that the pentanal cluster would go through ISC from the S_1 to the T_1 state before undergoing any photochemical changes. It was further assumed that ISC (eventually) takes place at the geometries where the S_1–T_1 energy gap is the smallest. Therefore, during the molecular dynamics simulation in the ground state, the S_1 and T_1 energies were computed, and the S_1–T_1 energy gap was calculated. The observed S_1–T_1 energy gap range was 0.36–0.69 eV for the pentanal cluster simulations, and these geometries were then used as the starting point for the triplet state dynamics. This approach is similar to our previous approach,[26,46] except that the step involving excited-state dynamics on the S_1 surface was skipped. Examination of the trajectories shows that the omission of this step is justified, since the system does not gain or lose almost any kinetic energy during the molecular dynamics on the S_1 surface. In the bare pentanal, the velocity distribution at the crossing point after dynamics in the S_1 state is similar to the initial velocity distribution and the average kinetic energy per mode corresponds to about k_BT. We note that the velocity distribution obtained from the ground state simulation is of the same value. This has been checked in over a hundred trajectories. Additionally the minor differences in the velocity distribution cannot lead to the major effect in reactions as seen in this study. Therefore our approach is practically similar to ref. 26.

The important point in our approach is the identification of the most probable crossing structures. The reader is referred to ref. 26 and 46 for a more detailed justification of this approach. The selected S_1–T_1 crossing geometries and atomic velocities were used as the starting conditions for propagating the dynamics on the T_1 surface. Our approach involves an assumption that no additional internal energy is gained by the transfer from the S_1 to T_1 surface. On the T_1 surface, the molecular dynamics simulation using the OM2 potential energy surface was invoked. Ref. 26 gives a detailed justification of why only the dynamics on the T_1 surface is needed for this simulation. Briefly, we have not observed any reactions on the S_1 surface with and without non-adiabatic surface hopping. Non-adiabatic surface hopping is not expected to occur in the simulation time frame. We note that a similar approach has also been used to investigate the dynamics starting from conical intersection on top of the reaction barrier on the excited states.[59,60]

(c) Experimental approach

Experiments were done by photolyzing undecanal (a straight-chain aliphatic C11 aldehyde), which conveniently adopts a liquid state under standard conditions. A sample cell with 1 inch diameter calcium fluoride windows and an adjustable (10–1000 μm) path length from Harrick Scientific was used in these experiments. Light traveled from a xenon arc lamp through a 295 nm long pass filter and a collimating lens to the sample cell. Pure liquid undecanal samples were photolyzed, dissolved in methylene chloride ($\sim 10^{-4}$ M), and analyzed using a Thermo Trace electron impact gas chromatography mass spectrometer (GCMS) to identify the reaction products.

III. Results and discussion

(a) Ground state simulation

Fig. 1 shows a structure of the cluster of five pentanal molecules optimized using the OM2 semiempirical method in conjunction with dispersion corrections. Before the optimization, we aligned all the pentanal molecules such that the aldehyde groups pointed in the same direction. The dispersion interaction is critical to the stability of the cluster; without it pentanal molecules were found to evaporate from the cluster within 10 ps simulation time. With the dispersion forces included, the structure of the cluster did not change much during the timescale of the simulations; the cluster can be described as ''solid-like'' rather than ''liquid-like''. While the optimized structure found may not be that of the global minimum, it corresponds at least to a low-energy minimum since it remains stable in the ground-state simulation at 300 K.

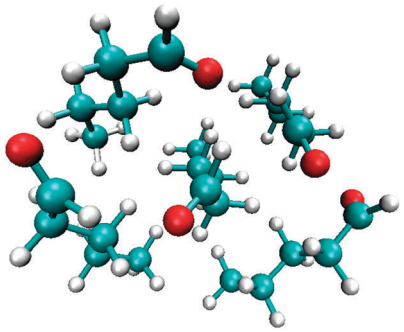

Fig. 1 The structure of the pentanal cluster optimized using OM2 with dispersion corrections.

(b) Triplet-state dynamics

Schemes 1 and 2 summarize all the reactions observed in the triplet-state molecular dynamics simulations. Table 1 contains information on the yields and average timescales of these reactions. Scheme 1 compiles the Norrish type reactions along with secondary processes that in some cases follow. Reaction 1a is the first step of the Norrish type I reaction, namely the C–C_α bond cleavage resulting in a butyl radical and a formyl radical.

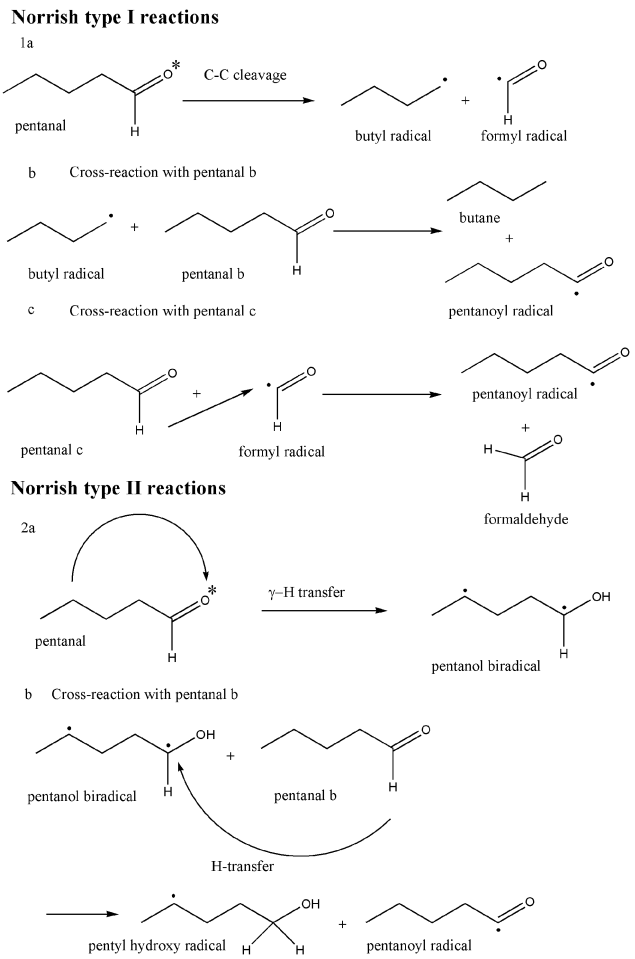

Scheme 1 Norrish type I and II reactions and following secondary intermolecular reactions observed in the molecular dynamics simulations.

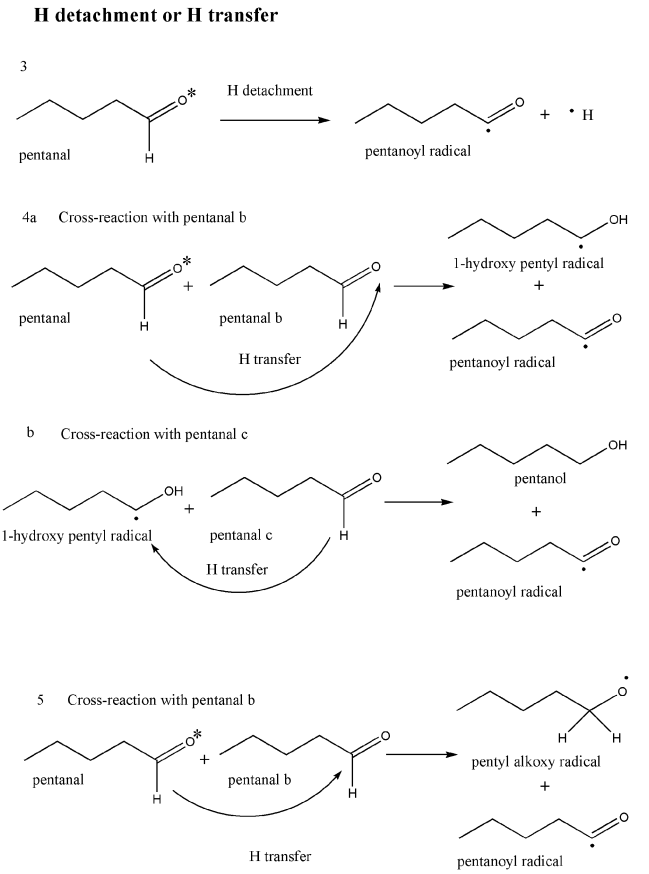

Scheme 2 H-atom detachment and H-atom transfer reactions and following secondary intermolecular reactions observed in the molecular dynamics simulations.

Table 1 Percentage and average timescales of the different processes observed during 100 ps simulation time

Reaction scheme number	% of total number of trajectories	Average reaction time (ps)	Monomeric or cross reaction
1a	9	13	Monomeric
1a + b	7	13	Cross reaction
1a + b + c	1	0.4	Cross reaction
2a	1	23	Monomeric
2a + b	3	23	Cross reaction
3	5	Immediately	Monomeric
4a	24	50	Cross reaction
4a + b	4	24	Cross reaction
5	1	61	Cross reaction

This reaction has also been observed in the bare pentanal molecule. Reaction 1b is the secondary reaction following the C–C_α cleavage. The butyl radical reacts with a second pentanal molecule to yield butane and a pentanoyl radical. Additionally, the formyl radical can further react with another pentanal to form a pentanoyl radical and formaldehyde. A total of 17% of the trajectories start with the Norrish type I reaction (Table 1), very similar to the yield observed for the bare pentanal (14%).

Reaction 2a is the first step of the Norrish type II reaction, namely an intramolecular H-atom transfer from the C_γ to the

carbonyl group. The pentanol biradical created by the Norrish type II reaction continues to react (2b) with a second pentanal molecule to create a pentyl hydroxy radical and a pentanoyl radical. The Norrish type II reaction was the dominant pathway in the bare pentanal (27%), but in the cluster it plays a minor role (4%). A possible explanation for the suppression of this process in the cluster is that it requires a substantial change of configuration in order to reach the relevant transition state. Structural constraints introduced by the neighboring molecules and loss of energy in vibrational energy transfer suppress the Norrish II channel and favors cross-reactions instead (see the following discussion).

Scheme 2 summarizes other types of reactions occurring in the simulations. The common starting reaction is the H-atom detachment from the aldehydic carbon. The H-atom detachment was described in our recent study on the bare pentanal as a minor event (1%), as well as in the experimental studies.[61,62] In a small number of trajectories (5%) the H atom evaporates from the cluster on a femtosecond timescale (reaction 3) and is not involved in further reactions. In such cases, a pentanoyl radical is the terminal product.

However, the H-atom transfer to another pentanal molecule plays a major role in the reactions observed in the cluster simulations. In all the other trajectories, the H atom is directly transferred to another pentanal molecule or a secondary radical. The most probable reaction (28%) starts with an H-atom transfer to the oxygen of another pentanal molecule, to form two new radicals, a 1-hydroxy pentyl radical and a pentanoyl radical (reaction 4a). The 1-hydroxy pentyl radical may accept, in a secondary reaction, another H atom from a different pentanal to form pentanol and a pentanoyl radical (reaction 4b). A minor pathway shows the H-atom transfer to the carbon of the carbonyl group, creating the pentyl alkoxy radical and the pentanoyl radical (reaction 5). In total, the combined yield of cross-reactions was three times higher than the combined yield of unimolecular reactions on the simulation timescale of 100 ps. It can be expected that an elongation of the simulation time or increase in the cluster size would increase the effective yield of the secondary reactions even further, and produce additional radicals and molecules. But clearly, a rich photochemistry is already evident even in a small cluster and on a relatively short simulation timescales.

Fig. 2 shows the snapshots of the reaction pathways 1a + b + c as an example of the rich photochemistry found here. The first step promptly occurring in about 0.36 ps is the C–C_α bond cleavage. Some 50 ps later, a favorable configuration is found to enable the H-atom transfer from the CHO group to the butyl radical, forming butane and a pentanoyl radical. A third pentanal at about 89.4 ps loses its H atom to the formyl radical resulting in formaldehyde and another pentanoyl radical.

Comparison of the reaction timescales observed in the pentanal cluster and in the bare pentanal provides additional insights into the mechanism. Fig. 3 shows a histogram summarizing the times of occurrence of unimolecular reactions for the bare pentanal (a), for the pentanal cluster (b), and the cross-reactions in the pentanal cluster (c).

The unimolecular reactions observed in the bare pentanal molecule occur almost uniformly over the whole timescale of 100 ps. In contrast, the same unimolecular reactions in the pentanal cluster are much more pronounced in the beginning of the simulation time window. This suggests that unimolecular reactions can only prevail if the excited molecule is optimally oriented at the beginning of the simulation; if it is not, cross-reactions become more probable.

The orientation of the molecules has a large effect on the reactions observed here. Only certain orientations allow an H-atom transfer to neighboring molecules. In addition, the cross-molecular processes play a bigger role on longer timescales. The ultrafast processes, especially the Norrish type I reaction, are less affected by the initial orientation of the molecules. The cross-reactions observed in the cluster are distributed almost equally over the whole simulation timescale.

It is also noteworthy to compare the unreactive processes in the bare pentanal molecule *vs.* the pentanal cluster. For the bare pentanal molecule, 58% of the trajectories on the timescale of 100 ps were unreactive.

This number is reduced to 45% in the pentanal cluster. It can be concluded that the cluster environment enhances the number of reactive trajectories. It can be expected that longer

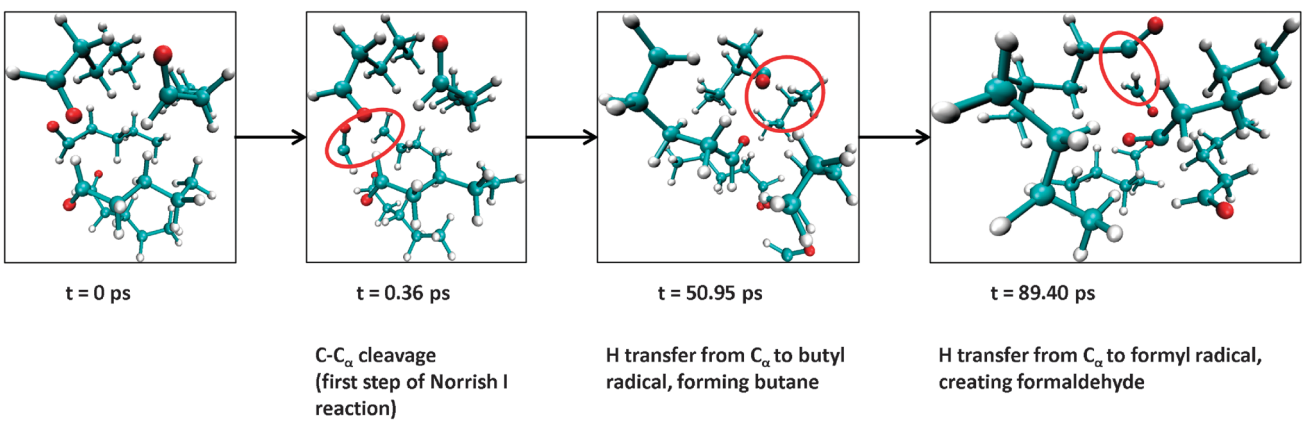

Fig. 2 Snapshots of the reaction pathway 1a + b + c.

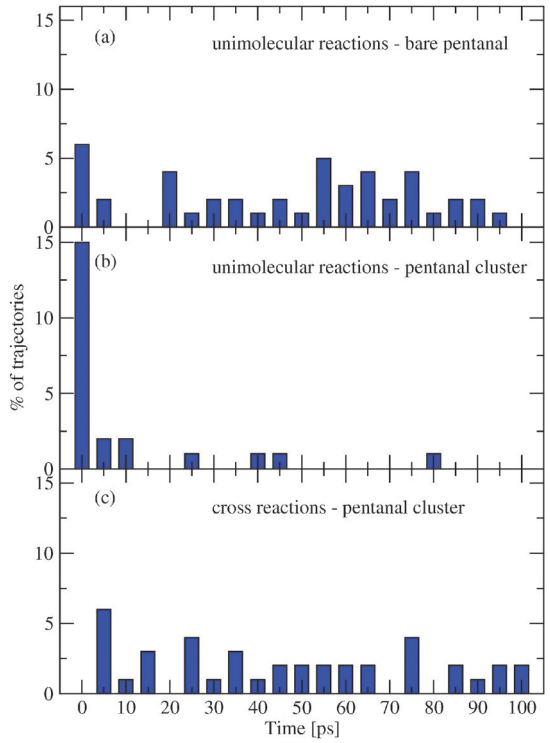

Fig. 3 Histograms of the (a) number of unimolecular processes in a bare pentanal molecule *vs.* time, (b) unimolecular processes of a pentanal molecule embedded in the pentanal cluster *vs.* time and (c) cross reactions in the pentanal cluster *vs.* time.

simulation timescales or larger clusters should increase the percentage of reactive trajectories even more.

(c) Experimental evidence and implications

Experimental results on a longer aldehyde, undecanal, qualitatively support the predicted importance of cross-reaction mechanisms in photolysis of aliphatic aldehydes. Norrish type I and II reactions[63] are well known for aldehydes and can be expected to form products, which are consistent with the simulated processes. In particular, the Norrish type I product decane (an analog of the butane product in the simulation) was detected in the photolysis of liquid undecanal by GCMS. Although decane may directly form from the molecular dissociation channel (process A in the Introduction section), the condensed-phase environment offers a more probable pathway *via* an H-atom abstraction by the initially formed decyl radical from another undecanal molecule.[3,64–69] A Norrish type II product 1-nonene (corresponding to 1-propene in the pentanal photolysis case) was also observed. This product has not appeared in our simulation, but its precursor (pentanol biradical) was created after the first step of Norrish II reaction. Presumably, the actual Norrish II splitting step (eqn (C)) occurs on a much longer time scale than the simulation can realistically handle. There was also clear evidence in the GCMS chromatograms of other cross-molecular reaction products. For example, two aldehyde molecules may undergo autoinhibition *via* an intermolecular H-atom abstraction to form an undecanoyl radical and an α-hydroxy undecanol radical (similar to the pentanoyl and α-hydroxy pentanol radicals seen in reaction 4a).[67] The latter radical may recombine with the Norrish type I decyl radical to form the experimentally observed photoproducts 11-heneicosanone and 11-heneicosanol. These products are strong indicators of free radical reactions in the condensed-phase. For example, Kossanyi *et al.* photolyzed benzophenone in an excess of butanal and proposed that the excited benzophenone could abstract an H atom from butanal.

It was noted that another butanal molecule could abstract an H atom from the protonated benzophenone radical to give the starting ketone and proceed in a "chain-like" reaction. It was emphasized that if only these two processes occurred, then the benzophenone photolysis quantum yield should have been less than 1, but was in fact 1.4 owing to the additional radical reactions.

Kossanyi *et al.* explained that the larger benzophenone photolysis quantum yield would arise from cross-molecular reactions of radicals with the ground state benzophenone.[68] Similar condensation products in the form of RCOR and RCHOHR have been identified in continuous laser photolysis experiments of pure pentanal by Paquet *et al.*, where the starting aldehyde is RCOH.[67] Other minor secondary photolysis products of undecanal were also observed, but their definite identification requires further analysis.

IV. Conclusions

The following conclusions can be drawn from this study. First of all, a rich photochemistry is observed from the photoexcitation of a pentanal cluster already in the short timescale of 100 ps. In particular, different free radicals are formed, as well as molecules. Intramolecular reactions, such as the Norrish type II splitting, are partly suppressed in the cluster, whereas cross-reactions, especially an H-atom transfer between two different monomeric units of the cluster are pronounced. Nearly three quarters of all reactive events correspond to the cross-reactions. Therefore, it is very important to address the issue of cross-reactions in theoretical and experimental studies of organic photochemistry, a topic of high importance, but also of high complexity. Theoretically, the simulation can be extended to larger and more complex systems. The ultimate goal is to adequately simulate photochemical processes occurring in complex environmental systems and involving molecules with multiple other functional groups in addition to the aldehyde group considered in this work. We trust that the small molecular cluster approach presented here will be instrumental in predicting photochemical mechanisms in these systems.

The rich photochemistry can have a major effect on the atmosphere, especially on the molecular composition of organic aerosols exposed to sunlight. For example, it has been proposed that photolysis of carbonyls represents an important mechanism of aging of secondary organic aerosols.[70] The occurrence of cross-reactions of photoexcited carbonyls in the condensed-phase environment of an organic aerosol particle may significantly increase the efficiency of aerosol photolysis. Photochemical behavior of larger carbonyl compounds, which reside in the condensed-phase because of their low volatility, cannot be

reliably predicted from our knowledge of gas-phase photochemistry of carbonyls without taking cross-reactions into account.

From the methodological point of view, this study demonstrates advantages of the simulation using a semiempirical potential energy surface. The system size is too large for employing a more accurate methodology. The methodology used here enables us to study photochemistry of sufficiently complicated clusters, which are large enough to provide important insights into the reaction dynamics in condensed phases. We, therefore, suggest further applications using the current methodology for other clusters, where complex reactions are foreseen.

Conflicts of interest

The authors declare no competing financial interests.

Acknowledgements

This research was supported by the Israel Science Foundation, Grant No. 172/12 and by NSF (USA) through EMSI at UC Irvine (Grant No. CHE-0909227).

References

1 P. J. Robinson and K. A. Holbrook, *Unimolecular Reactions*, Wiley, New York, 1973.
2 R. G. Gilbert and S. C. Smith, *Theory of Unimolecular and Recombination Reactions*, Blackwell, Oxford, 1990.
3 N. J. Turro, V. Ramamurthy and J. C. Scaiano, *Modern Molecular Photochemistry of Organic Molecules*, University Science Books, Sausalito, CA, 2010.
4 V. A. Apkarian and N. Schwentner, *Chem. Rev.*, 1999, **99**, 1481.
5 R. B. Gerber, A. B. Mccoy and A. Garciavela, *Annu. Rev. Phys. Chem.*, 1994, **45**, 275.
6 A. I. Krylov and R. B. Gerber, *J. Chem. Phys.*, 1997, **106**, 6574.
7 R. Alimi and R. B. Gerber, *Phys. Rev. Lett.*, 1990, **64**, 1453.
8 S. Buelow, M. Noble, G. Radhakrishnan, H. Reisler, C. Wittig and G. Hancock, *J. Phys. Chem.*, 1986, **90**, 1015.
9 S. Buelow, G. Radhakrishnan, J. Catanzarite and C. Wittig, *J. Chem. Phys.*, 1985, **83**, 444.
10 N. F. Scherer, L. R. Khundkar, R. B. Bernstein and A. H. Zewail, *J. Chem. Phys.*, 1987, **87**, 1451.
11 N. F. Scherer, C. Sipes, R. B. Bernstein and A. H. Zewail, *J. Chem. Phys.*, 1990, **92**, 5239.
12 A. B. McCoy, Y. Hurwitz and R. B. Gerber, *J. Phys. Chem.*, 1993, **97**, 12516.
13 B. J. Finlayson-Pitts and J. N. J. Pitts, *Chemistry of the Upper and Lower Atmosphere*, Academic Press, 2000.
14 E. K. C. Lee and R. S. Lewis, *Adv. Photochem.*, 1980, **12**, 1.
15 Y. Kurosaki, *THEOCHEM*, 2008, **850**, 9.
16 G. A. Amaral, A. Arregui, L. Rubio-Lago, J. D. Rodriguez and L. Banares, *J. Chem. Phys.*, 2010, **133**, 064303.
17 M. A. Blitz, D. E. Heard and M. J. Pilling, *J. Photochem. Photobiol., A*, 2005, **176**, 107.
18 M. A. Buntine, C. Lee and G. F. Metha, *Phys. Chem. Chem. Phys.*, 2004, **6**, 688.
19 X. B. Chen and W. H. Fang, *Chem. Phys. Lett.*, 2002, **361**, 473.
20 M. N. D. S. Cordeiro, E. Martinez-Nunez, A. Fernandez-Ramos and S. A. Vazquez, *Chem. Phys. Lett.*, 2003, **381**, 37.
21 T. J. Cronin and L. Zhu, *J. Phys. Chem. A*, 1998, **102**, 10274.
22 B. N. Fu, B. C. Shepler and J. M. Bowman, *J. Am. Chem. Soc.*, 2011, **133**, 7957.
23 J. Matthews, A. Sinha and J. S. Francisco, *J. Chem. Phys.*, 2005, **122**, 221101.
24 G. F. Metha, A. C. Terentis and S. H. Kable, *J. Phys. Chem. A*, 2002, **106**, 5817.
25 S. E. Paulson, D. L. Liu, G. E. Orzechowska, L. M. Campos and K. N. Houk, *J. Org. Chem.*, 2006, **71**, 6403.
26 D. Shemesh, Z. G. Lan and R. B. Gerber, *J. Phys. Chem. A*, 2013, **117**, 11711.
27 Y. X. Tang and L. Zhu, *J. Phys. Chem. A*, 2004, **108**, 8307.
28 L. R. Valachovic, M. F. Tuchler, M. Dulligan, T. Droz-Georget, M. Zyrianov, A. Kolessov, H. Reisler and C. Wittig, *J. Chem. Phys.*, 2000, **112**, 2752.
29 L. Zhu, T. Cronin and A. Narang, *J. Phys. Chem. A*, 1999, **103**, 7248.
30 L. Zhu, Y. X. Tang, Y. Q. Chen and T. Cronin, *Spectrosc. Lett.*, 2009, **42**, 467.
31 J. Tadic, I. Juranic and G. K. Moortgat, *Molecules*, 2001, **6**, 287.
32 J. Tadic, I. Juranic and G. K. Moortgat, *J. Photochem. Photobiol., A*, 2001, **143**, 169.
33 J. M. Tadic, I. O. Juranic and G. K. Moortgat, *J. Chem. Soc., Perkin Trans. 2*, 2002, 135.
34 J. M. Tadic, G. K. Moortgat, P. P. Bera, M. Loewenstein, E. L. Yates and T. J. Lee, *J. Phys. Chem. A*, 2012, **116**, 5830.
35 J. M. Tadic, L. Xu, K. N. Houk and G. K. Moortgat, *J. Org. Chem.*, 2011, **76**, 1614.
36 M. Ben-Nun, J. Quenneville and T. J. Martinez, *J. Phys. Chem. A*, 2000, **104**, 5161.
37 V. S. Batista and D. F. Coker, *J. Chem. Phys.*, 1996, **105**, 4033.
38 Y. A. Bernard, Y. H. Shao and A. I. Krylov, *J. Chem. Phys.*, 2012, **136**, 204103.
39 N. L. Doltsinis and D. Marx, *Phys. Rev. Lett.*, 2002, **88**, 166402.
40 W. Domcke and D. R. Yarkony, *Annu. Rev. Phys. Chem.*, 2012, **63**, 325.
41 M. Etinski, T. Fleig and C. A. Marian, *J. Phys. Chem. A*, 2009, **113**, 11809.
42 L. M. Frutos, T. Andruniow, F. Santoro, N. Ferre and M. Olivucci, *Proc. Natl. Acad. Sci. U. S. A.*, 2007, **104**, 7764.
43 L. Martinez-Fernandez, I. Corral, G. Granucci and M. Persico, *Chem. Sci.*, 2014, **5**, 1336.
44 D. Shemesh and R. B. Gerber, *Mol. Phys.*, 2012, **110**, 605.
45 S. A. Epstein, D. Shemesh, V. T. Tran, S. A. Nizkorodov and R. B. Gerber, *J. Phys. Chem. A*, 2012, **116**, 6068.
46 H. Lignell, S. A. Epstein, M. R. Marvin, D. Shemesh, R. B. Gerber and S. A. Nizkorodov, *J. Phys. Chem. A*, 2013, **117**, 12930.
47 W. Weber and W. Thiel, *Theor. Chem. Acc.*, 2000, **103**, 495.

48 A. Koslowski, M. E. Beck and W. Thiel, *J. Comput. Chem.*, 2003, **24**, 714.
49 J. J. P. Stewart, *J. Comput. Chem.*, 1989, **10**, 209.
50 D. Shemesh and R. B. Gerber, *J. Chem. Phys.*, 2005, **122**, 241104.
51 D. Shemesh and R. B. Gerber, *J. Phys. Chem. A*, 2006, **110**, 8401.
52 D. Shemesh, G. M. Chaban and R. B. Gerber, *J. Phys. Chem. A*, 2004, **108**, 11477.
53 D. Shemesh, R. Baer, T. Seideman and R. B. Gerber, *J. Chem. Phys.*, 2005, **122**, 184704.
54 Y. Miller, G. M. Chaban, B. J. Finlayson-Pitts and R. B. Gerber, *J. Phys. Chem. A*, 2006, **110**, 5342.
55 Y. Miller and R. B. Gerber, *J. Am. Chem. Soc.*, 2006, **128**, 9594.
56 Q. Wu and W. T. Yang, *J. Chem. Phys.*, 2002, **116**, 515.
57 W. Thiel, *MNDO program, version 6.1*, Mülheim an der Ruhr, Germany, 2007.
58 E. Fabiano, T. W. Keal and W. Thiel, *Chem. Phys.*, 2008, **349**, 334.
59 B. Sellner, M. Barbatti and H. Lischka, *J. Chem. Phys.*, 2009, **131**, 024312.
60 D. Asturiol, B. Lasorne, G. A. Worth, M. A. Robb and L. Blancafort, *Phys. Chem. Chem. Phys.*, 2010, **12**, 4949.
61 J. G. Calvert and J. N. Pitts, *Photochemistry*, John Wiley, New York, 1966.
62 P. Warneck and G. K. Moortgat, *Atmos. Environ.*, 2012, **62**, 153.
63 R. G. W. Norrish and C. H. Bamford, *Nature*, 1936, 1016.
64 P. A. Leighton, *Photochemistry of air pollution*, Academic Press, New York, 1961.
65 T. Fujisawa, B. M. Monroe and G. S. Hammond, *J. Am. Chem. Soc.*, 1970, **92**, 542.
66 D. I. Schuster and P. B. Karp, *J. Photochem.*, 1980, **12**, 333.
67 P. Paquet, R. Fellous, R. Stringat and G. Fabre, *Tetrahedron Lett.*, 1992, **33**, 485.
68 J. Kossanyi, S. Sabbah, P. Chaquin and J. C. Ronfartharet, *Tetrahedron*, 1981, **37**, 3307.
69 C. W. Funke and H. Cerfontain, *J. Chem. Soc., Perkin Trans. 2*, 1976, 669.
70 S. A. Mang, D. K. Henricksen, A. P. Bateman, M. P. S. Andersen, D. R. Blake and S. A. Nizkorodov, *J. Phys. Chem. A*, 2008, **112**, 8337.
71 R. B. Gerber, D. Shemesh, M. E. Varner, J. Kalinowski and B. Hirshberg, *Phys. Chem. Chem. Phys.*, 2014, **16**, 9760.

